Molecular Structure in Crystal Aggregates of Linear Polyethylene

By R. D. BURBANK

(Manuscript received July 6, 1960)

Crystal aggregates of linear polyethylene have been studied in the electron microscope. Twinning has been observed to occur across (530) planes, and possibly across (120) planes. Crystal morphologies have been observed which exhibit (530) and (540) faces. Electron interference effects have been observed which give rise to contrast lines and figures which frequently are parallel to crystallographic directions. These observations, and those of others, have been interpreted in terms of recently proposed ideas on molecular chain folding. It is suggested that chain folds may lie in a variety of fold planes or fold surfaces which are normal, or nearly normal, to the crystal lamellae. It is shown that a continuity of fold structure is necessary and possible across a wide variety of boundaries delineating regions of different fold structure. It is shown that these structural concepts are compatible with recently proposed ideas on the growth of lamellar polymer crystals and can suggest new details of the growth process.

I. INTRODUCTION

A variety of properties — chemical, electrical and mechanical — have combined to make polyethylene an extremely important material in the telephone system. The sustained attempt to improve the characteristics of polyethylene for different applications depends very much on further understanding of the fundamental structure and behavior of high polymer molecules. Unfortunately, high polymers manifest a tremendous range of structural organization, almost comparable in complexity with the simpler biological systems. Any simplification that can be obtained in the structural organization of a polymer is of inestimable value if the material is to be used for fundamental study.

The discovery that well-developed crystals of linear polymers can readily be obtained from dilute solutions was made independently in several laboratories.[1,2,3] A lamellar-like habit and spiral growth terraces

were found to be ubiquitous features of the crystals. It was recognized that three-dimensional crystal growth must occur by the Frank screw-dislocation mechanism. In addition, Keller[2] concluded that the molecules in linear polyethylene crystals must sharply fold back on themselves with a chain length of about 100 angstroms between folds. A similar deduction concerning molecular folding in films of gutta percha[4] had long been forgotten until Keller called attention to it. Keller and O'Connor[5] postulated that the molecular folds in linear polyethylene lie in (110) planes in crystals which are bounded by (110) faces. They also obtained electron diffraction patterns showing twinning on (110) planes.

With improved techniques to minimize electron beam damage, Agar, Frank and Keller[6] obtained a profusion of electron interference effects with linear polyethylene crystals. Moiré fringes, Bragg extinction contours, and other contrast effects were obtained in bright field and dark field illumination. The surface morphology of some crystals bounded by (110) faces indicated a distinct division into four quadrants. It was proposed that the molecular folds are arranged in four different sets of (110) planes in the various quadrants. Consistent with this proposal was the observation that adjacent quadrants satisfied different conditions of diffraction. Meanwhile, Sella and Trillat[7] reported electron diffraction patterns showing twinning of polyethylene on both (110) and (310) planes, a variety of multiple diffraction effects and striking contrast periodicities in microfibrils.

Bassett, Frank and Keller[8] and Niegisch[9] independently proposed that lamellae of linear polyethylene grow as hollow, nonplanar pyramids which collapse upon drying to leave planar lamellae with a characteristic surface morphology involving a central triangular pleat or fold. Bassett et al. observed that in crystals bounded by both (110) and (100) faces a structure may be observed in the electron microscope with dark field illumination which divides the crystal into six sectors. It was suggested that, in the sectors bounded by (100) faces, the molecular folds were parallel to (100) planes. This concept was supported by the observation that the (100) sectors have a different melting point or transformation temperature than the rest of the crystal.

Niegisch and Swan[10] and Reneker and Geil[11] observed polyethylene lamellae which have folded over along the short diagonal parallel to the *b* axis. The fold edge is angular rather than straight. This is consistent with a hollow pyramid interpretation and permits a direct measurement of the inclination of such a pyramid to the basal plane. Both Niegisch and Swan and Reneker and Geil have shown that there is an arrangement of folds in (110) planes which forms a (111) surface. The hollow pyramid

formed by four (111) surfaces has an inclination in agreement with that deduced from observations of folded lamellae. Reneker and Geil[11] have extended the argument considerably, however. They show that there are other fold arrangements in (110) planes which form (001) or (112) surfaces. They have interpreted other lamellar morphologies in which corrugations along (310) planes and (530) planes are prominent.

Recently the writer had access to a portion of the operating time on a Siemens Elmiskop I electron microscope for a period of several months. A number of observations were made on crystal aggregates of linear polyethylene. Certain crystallographic relationships were found that have been interpreted in terms of the recently developed ideas on fold structures. Many speculations concerning fold structures have been made in a systematic way that should be useful in discussing molecular configurations of crystalline polymers in general.

II. EXPERIMENTAL

The linear polyethylene used throughout was Marlex 50, melt index 6.0. Crystals were grown from xylene solutions at 0.04 and 0.07 per cent weight concentrations. Cooling rates were not carefully controlled. The heat under a small oil bath was simply removed and the solutions cooled to room temperature over a period of about 60 to 90 minutes. Specimens were prepared by stirring up the crystal-liquid suspension, removing a small quantity of suspension in a fine dropper, and depositing a few small drops on a specimen support. The specimen supports consisted of evaporated carbon films which were mounted on fine copper mesh.

Experimental details given by Agar et al.,[6] were most helpful as a guide to minimizing electron-beam damage in the Siemens Elmiskop I. The double condenser was used throughout the work. In general, one would not expect a reciprocity law to hold between intensity and time. Rather, one would expect low intensities and long times to produce less damage than high intensities and short times. Belavtseva[12] has verified this by experiment, and he has also found higher energy electrons to be less damaging. However, 100-kv electrons never gave as good contrast as 80-kv electrons. Consequently, 80-kv beams were used for most of the work. Best results were obtained with 100μ or 50μ condenser apertures, 50μ or 20μ objective apertures, 2500$\times$ magnification, completely defocused condensers and very long exposure times. Specimens exposed for a 3-minute dark field micrograph, 45-second diffraction pattern and 2-minute bright field micrograph still gave excellent interference effects. Instrumental stability appeared to be adequate at all times. Considerable darkroom adaption was necessary for the low intensities involved.

An interesting diffraction pattern obtained early in the investigation is illustrated in Fig. 1. Discounting some very fine spots which are clustered on (110) and (200) rings, all of the reflections can be accounted for by twinning on (530) and extensive double diffraction. The measured angle between the twinned lattices is 83°55′. Measurement was made with a circular measuring device capable of reading to 2.5′, such as is used for X-ray precession camera photographs. The calculated angle is 83°58′, assuming an a/b axial ratio of 1.5. The axial ratio was measured on all diffraction patterns, and angular relations were not sought unless the measured ratio was 1.5. As the crystals deteriorate in the electron beam the axial ratio increases and values up to 1.65 were observed. Axial ratio measurements could conceivably form an empirical yardstick for quantitative studies of electron beam damage. Fig. 2 is a bright-field micrograph of the (530) twins. Unfortunately, this specimen was destroyed in the beam. The crystals are "dead" and give no interference effects. There is a confused area in the center of the micrograph where both orientations are intergrown.

Fig. 3 is a bright-field micrograph of interpenetrant crystal growth. There are two large branches which form a cross. A smaller branch has

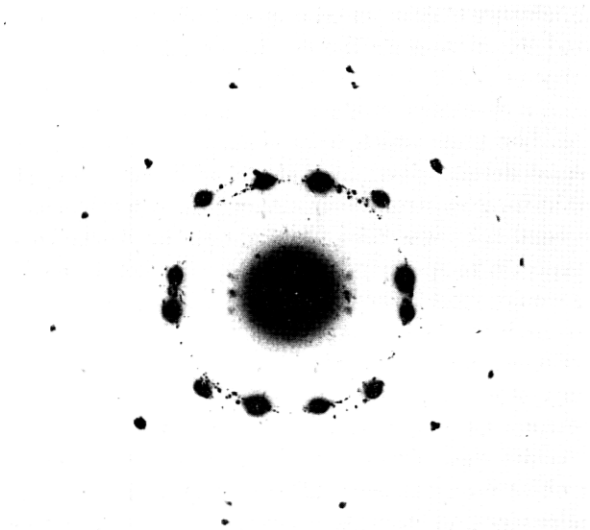

Fig. 1 — Electron diffraction pattern given by crystals twinned across (530) plane.

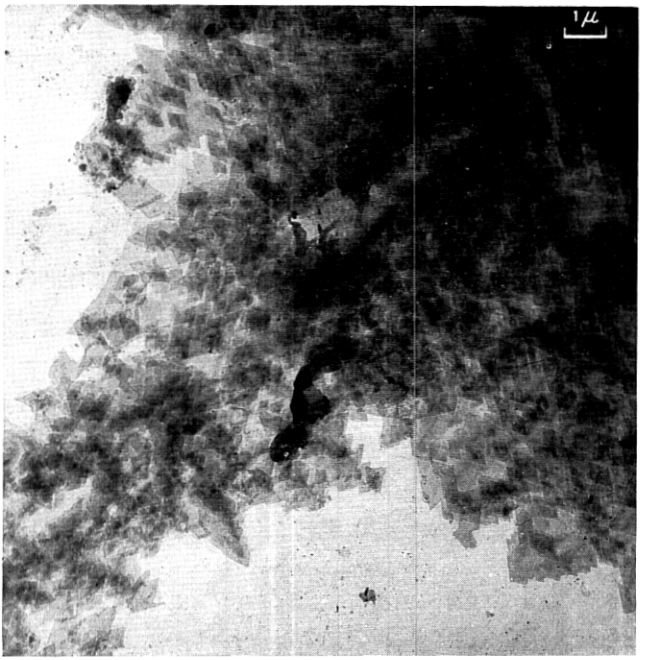

Fig. 2 — Bright-field micrograph of crystals twinned across (530) plane.

grown out from the upper right area of the cross. Fig. 4 is the diffraction pattern of this aggregate. Discounting a scattering of very fine spots, there are two intense arrays of reflections and a third array of moderate intensity. The measured angle between the lattices of intense spots is 68°40′. The calculated angle for (110) twinning is 67°2′. The measured angle between the lattice of moderate intensity and the right-hand lattice of high intensity is 35°22′. The calculated angle for (120) twinning is 36°38′. A variety of weaker reflections caused by double diffraction can be recognized. The crystals illustrated in Figs. 3 and 4 were obtained from 0.07 per cent xylene solution; all the other specimens under discussion were obtained from 0.04 per cent xylene solution.

Fig. 5 is a dark-field micrograph of a type of crystal aggregate which is very common in 0.04 per cent solutions. Many of the specimens illustrated by Agar et al.,[6] are of this type. Similar interference effects may be noted throughout. We should like to direct attention to the Bragg extinction contours which occur in profusion; they may appear as curves, loops, parallelograms, quadrilaterals, or straight lines. The contours of-

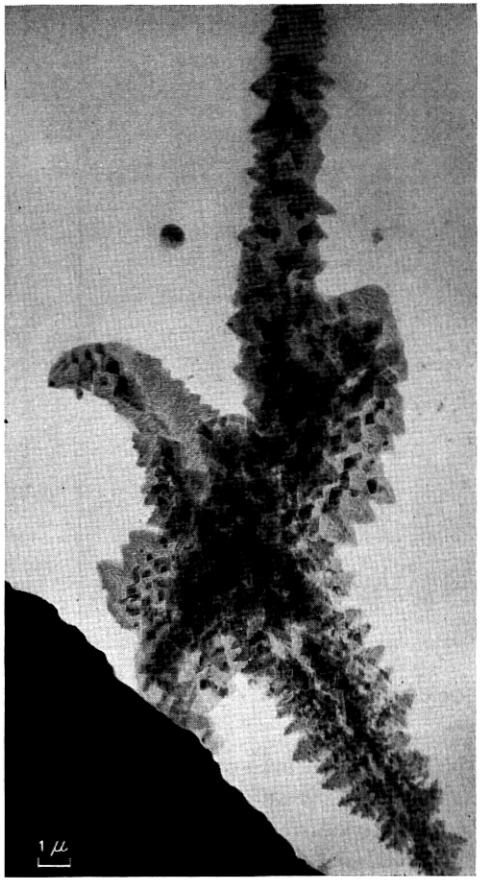

Fig. 3 — Bright-field micrograph of interpenetrant twin growth on (110) and (120) planes.

ten appear to be parallel to crystallographic planes. Certain patterns appear so consistently that it is difficult to ascribe them to mere accident. In the dark field of Fig. 6 some of the prominent loops in the upper part of the figure have sides which are parallel to (110) and (310) planes.

The dark field of Fig. 7 contains extinction contours that appear to be perfectly linear over distances of 5 to 10μ. Some of the crystallographic planes involved are illustrated in Fig. 8. There is one lamella which is bounded at a corner by (530) and ($\bar{5}$30) faces, while another lamella is bounded by (540) and ($\bar{5}$40) faces. These particular planes have been observed in a number of instances, either forming a corner or an edge

of a crystal aggregate. Thus, in the bright field of Fig. 9 there is a horizontal edge on the upper boundary which is parallel to ($\bar{5}40$).

Many diffraction patterns were recorded of crystal aggregates. Fine structure was invariably detected in the reflections if they were not exposed too heavily. The reflections appear at a casual glance to be more or less circular patches. Closer examination reveals a distinct mosaic structure in both radial and tangential directions. It is quite possible for moiré patterns to arise from tilts as well as rotations, and from combinations of both.[13] Tilts are likely to be operative in the cases of widely spaced fringes of 1000 angstroms or so.

III. CHAIN FOLDING — GENERAL CONSIDERATIONS

The types of chain folding discussed by Reneker and Geil[11] are given a simple representation in Fig. 10. A small rectangular patch of crystal is viewed along the *c* axis. The *a* axis is horizontal and the *b* axis vertical in the plane of the figure. (This crystallographic orientation is used throughout the remaining figures in this paper.) The molecular chains are normal to the plane of the figure. The molecules themselves are not indicated. The folds are situated in (110) planes. The distance that is

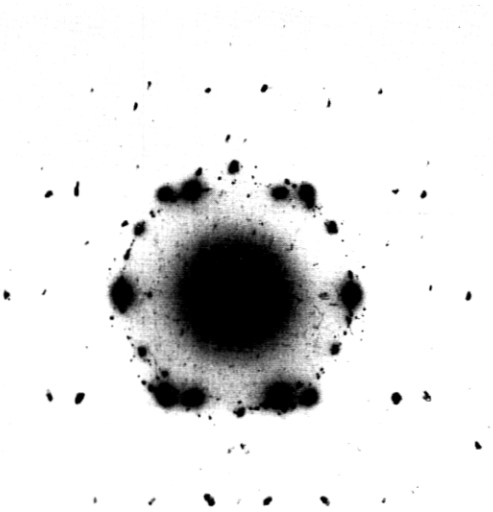

Fig. 4 — Electron diffraction pattern of crystals twinned on (110) and (120) planes.

Fig. 5 — Electron interference effects in dark-field micrograph of crystal aggregate. Note the profusion of extinction lines and curves.

bridged by a fold from one chain to another we call the fold width. When a fold is on the upper surface of the crystal it is indicated by a solid line in a (110) plane with a length equal to the fold width. When a fold is on the lower surface there is a blank space in a (110) plane with a length equal to the fold width. When all the folds are identical, containing say three carbon atoms per fold, the packing requirements put restrictions on the folds in successive fold planes.

According to Reneker and Geil,[11] in the arrangement of Fig. 10(a) the folds in successive fold planes must be displaced by nc. For $n = 0$, the folds form upper and lower crystal surfaces which are tangent to

(001) and (00$\bar{1}$). For $n = 1$, if the displacement is always in the same direction, the folds form upper and lower crystal surfaces which are tangent to (111) and ($\bar{1}\bar{1}\bar{1}$), or tangent to (11$\bar{1}$) and ($\bar{1}\bar{1}$1). In the arrangement of Fig. 10(b) the folds in successive fold planes must be displaced by $(n + \frac{1}{2})c$. For $n = 0$, if the displacement is always in the same direction, the upper and lower crystal surfaces are tangent to (112) and ($\bar{1}\bar{1}\bar{2}$), or tangent to (11$\bar{2}$) and $\bar{1}\bar{1}$2). For $n = 1$, if the displacement is always in the same direction, the upper and lower crystal surfaces are tangent to (332) and $\bar{3}\bar{3}\bar{2}$), or tangent to (33$\bar{2}$) and ($\bar{3}\bar{3}$2). Reneker and Geil also suggest that, if all the folds are not identical—for example, if there is an

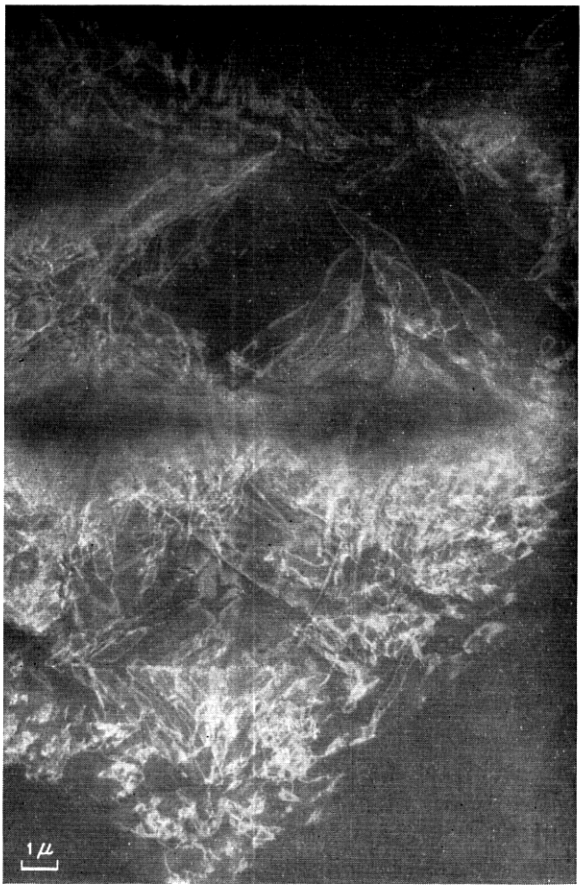

Fig. 6 — Dark-field micrograph. Some of the loops in the upper part of the figure have sides that are parallel to (110) and (310) planes.

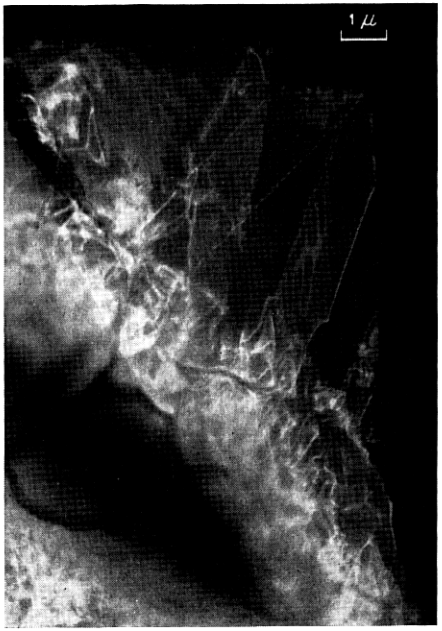

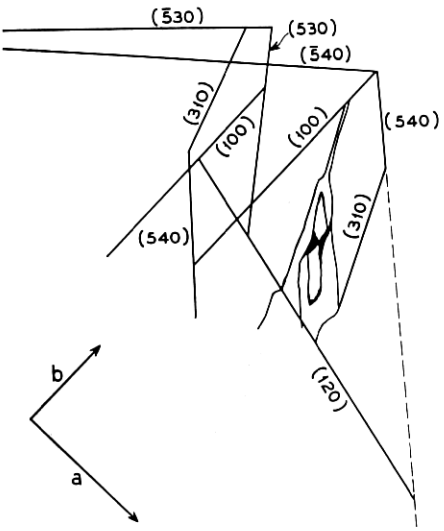

Fig. 7. Fig. 8.

Fig. 7 — Dark-field micrograph with linear extinction lines along well-defined directions.
Fig. 8 — Identification of some of the crystallographic planes observed in Fig 7.

alternation between three atom folds and five atom folds in successive fold planes—then surfaces tangent to (001) are possible.

In the remainder of this paper attention will be directed to two-dimensional aspects of chain folding. However, it should be clear from the preceding paragraph that whenever there is a change from one folding structure to another the crystal surfaces formed will generally change their inclination to the (001) plane. It is essential to develop some kind of notation to describe the various chain folding arrangements. The notation (110)[010] describes the folding in Fig. 10(a). The folds lie in (110) planes. The shortest vector displacement from a fold in one plane to an equivalent fold in the next plane is **b**, or, in our notation, [010]. There is another orientation of the Fig. 10(a) structure which can be written $(1\bar{1}0)[010]$. The symbol $(110)[\frac{1}{2}\frac{1}{2}0]$ describes the folding in Fig. 10(b). Here the shortest vector displacement from one fold to an equivalent in the next plane is $\mathbf{a}/2 + \mathbf{b}/2$, or $[\frac{1}{2}\frac{1}{2}0]$. There is obviously another orientation of the Fig. 10(b) structure, which can be written $(1\bar{1}0)[\frac{1}{2}\bar{\frac{1}{2}}0]$.

In principle, a crystal formed of (110)[010] folds might have a different melting point from a crystal formed of (110)[$\frac{1}{2}\frac{1}{2}$0] folds. In subsequent discussion we shall refer to such different arrangements as different phases. (The thermodynamicist, of course, would insist on additional criteria to define different phases.) The arrangements (110)[$\frac{1}{2}\frac{1}{2}$0] and (1$\bar{1}$0)[$\frac{1}{2}\frac{\bar{1}}{2}$0] do not represent different phases since they are mirror images of each other.

The observations of Bassett, Frank and Keller[8] on six-sector crystals with (100) faces indicate another type of fold structure. The most reasonable interpretation is that there are folds lying in planes parallel to the (100) faces. If the folds are situated in (200) planes the fold width increases by about 10 per cent relative to folds in (110) planes. Fig. 11 illustrates the folding structures that might be expected for this type

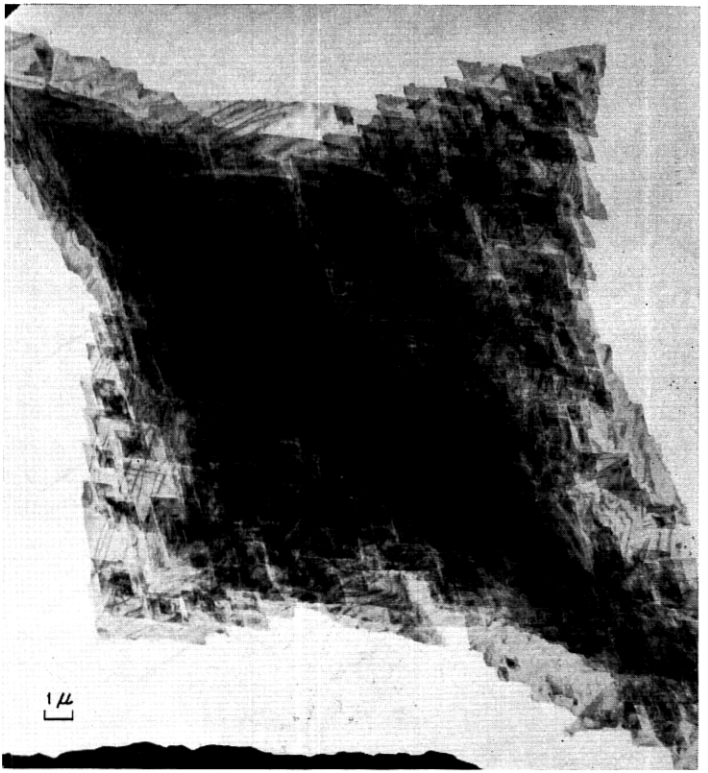

Fig. 9 — Bright field micrograph. Note horizontal edge on upper boundary which is parallel to ($\bar{5}$40).

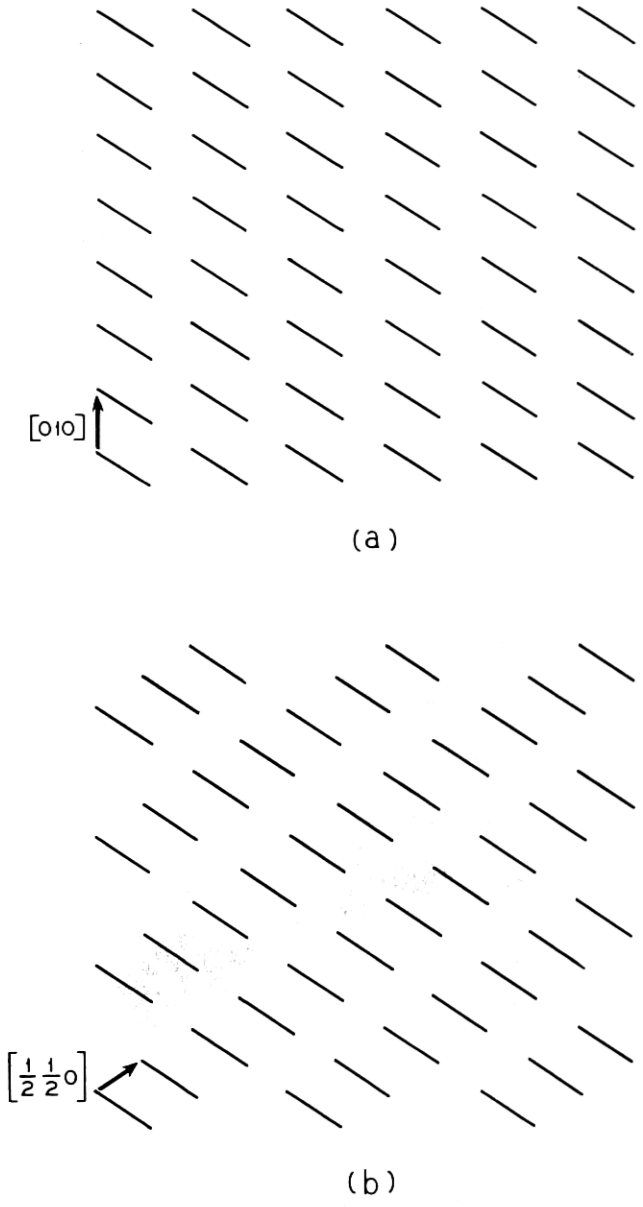

Fig. 10 — (a) (110)[010] fold structure; (b) (110)[½½0] fold structure. Crystal axes not illustrated but the a axis is horizontal, the b axis is vertical. This orientation is used in all the figures that follow.

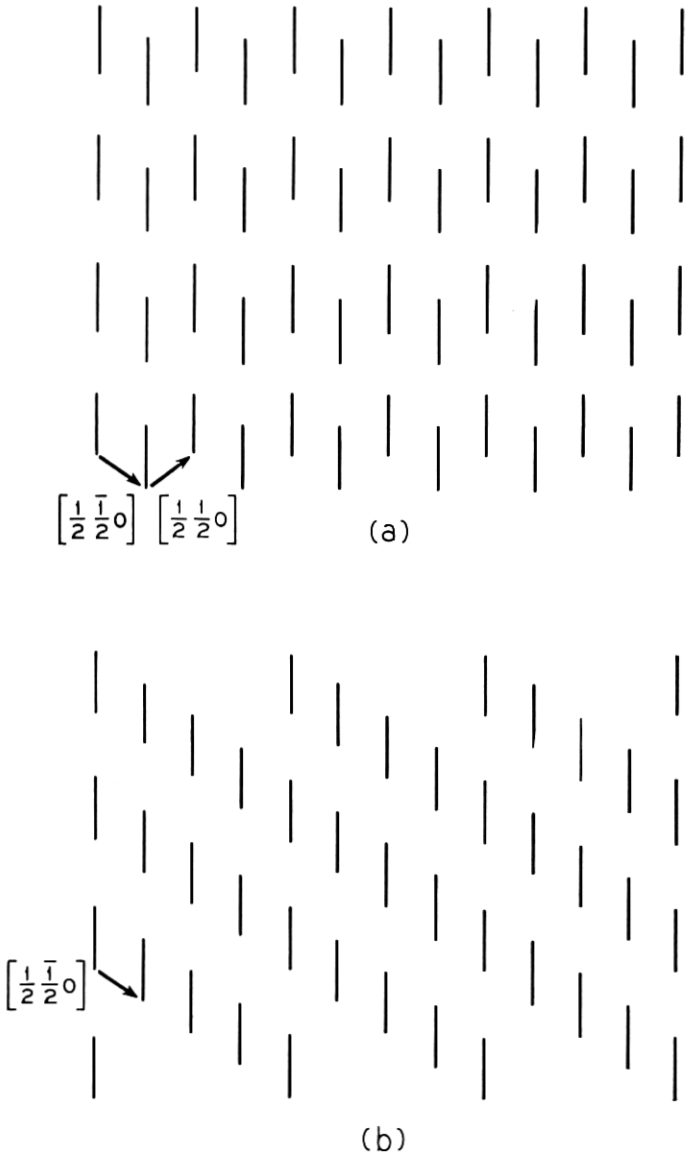

Fig. 11 — (a) (200)$[\frac{1}{2}\frac{1}{2}0]\cdot[\frac{1}{2}\frac{\bar{1}}{2}0]$ fold structure; (b) (200)$[\frac{1}{2}\frac{\bar{1}}{2}0]$ fold structure.

of fold. In Fig. 11(a) the structure can be written as (200)[$\frac{1}{2}\frac{1}{2}$0]·[$\frac{1}{2}\bar{\frac{1}{2}}$0], since the folds lie in (200) planes and the vector displacements of successive planes alternate between [$\frac{1}{2}\frac{1}{2}$0] and [$\frac{1}{2}\bar{\frac{1}{2}}$0]. In Fig. 11(b) the structure is written as (200)[$\frac{1}{2}\bar{\frac{1}{2}}$0]. There is another orientation of Fig. 11(b), which can be written as (200)[$\frac{1}{2}\frac{1}{2}$0].

In addition to the simple, repetitious fold structures there are many other possibilities that should be considered. Fig. 12(a) illustrates a situation that is analogous to the "twin boundaries" of Agar, Frank and Keller.[6] The more appropriate terms *fold domain* and *fold domain boundary* were introduced by Reneker and Geil[11] to describe the arrangement. There is a (110)[$\frac{1}{2}\frac{1}{2}$0] fold domain on the left, and a (1$\bar{1}$0)[$\frac{1}{2}\bar{\frac{1}{2}}$0] fold domain on the right. In the middle, parallel to (100), is a fold domain boundary. In this figure a few of the folds on the lower surface have been indicated by broken lines instead of blanks to emphasize that there is a *continuity* of the folds across the domain boundary. Such a continuity is certainly necessary to permit the formation of a domain boundary. Otherwise, one would have to impose the requirement that all the fold planes in a doman arbitrarily terminate at a common boundary. One might visualize a domain boundary as a place where, during crystal growth, growing fold planes change their orientation from one crystallographic direction to another. However, there is no discontinuity in the addition of molecules to the growing fold planes. The domains and the boundary of Fig. 12(a) might be symbolized (110)[$\frac{1}{2}\frac{1}{2}$0]:(1$\bar{1}$0)[$\frac{1}{2}\bar{\frac{1}{2}}$0].

Fig. 12(b) illustrates a different type of boundary, which would occur if the stacking arrangement of successive fold planes were altered. In the lower left of the figure the structure is (110)[010], and in the upper right it is (110)[$\frac{1}{2}\frac{1}{2}$0]. There is a boundary parallel to (110). In this instance it is a *phase boundary* that delineates two different structures and not merely two different orientations. Fig. 12(b) might be symbolized as (110)[010]:(110)[$\frac{1}{2}\frac{1}{2}$0].

In Fig. 13(a) a more general type of phase boundary is illustrated. In the lower left the structure is (200)$\frac{1}{2}\bar{\frac{1}{2}}$0]. The fold planes change orientation along a (110) boundary, as in a domain boundary. However, in this instance the change in orientation involves a change in fold structure to (1$\bar{1}$0)[$\frac{1}{2}\bar{\frac{1}{2}}$0]. Note that the element of continuity across the boundary prevails exactly as in the domain boundary of Fig. 12(a). The arrangement can be written as (200)[$\frac{1}{2}\bar{\frac{1}{2}}$0]:(1$\bar{1}$0)[$\frac{1}{2}\bar{\frac{1}{2}}$0].

In Fig. 13(b) a more complex possibility is suggested. The folds are not confined to a fold plane but lie in a corrugated surface, the *fold surface*. Successive folds in the fold surface alternate between (200) and (110) planes. Hence the fold surface might be symbolized as (200)·(110).

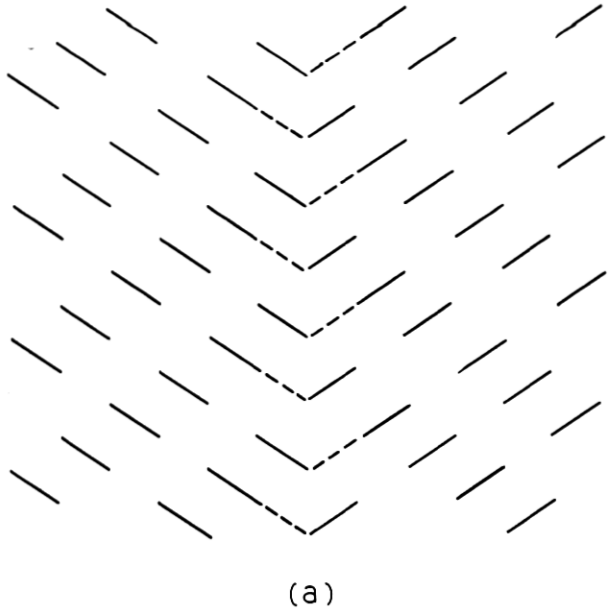

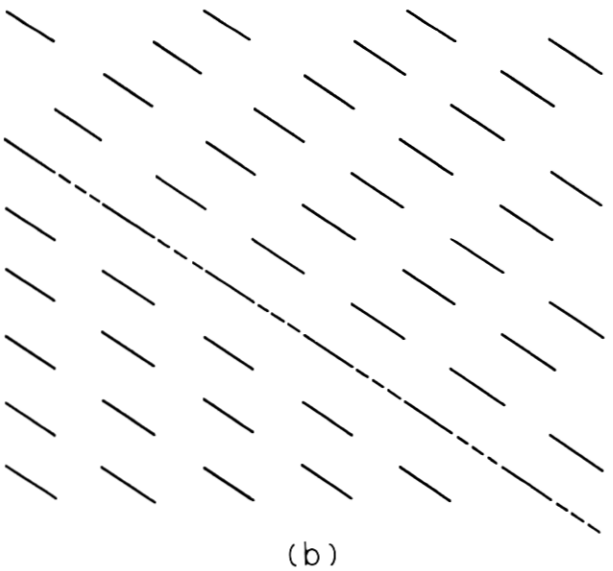

Fig. 12 — (a) $(110)[\frac{1}{2}\frac{1}{2}0]:(1\bar{1}0)[\frac{1}{2}\frac{\bar{1}}{2}0]$ domain boundary; (b) $(110)[010]:(110)[\frac{1}{2}\frac{1}{2}0]$ phase boundary.

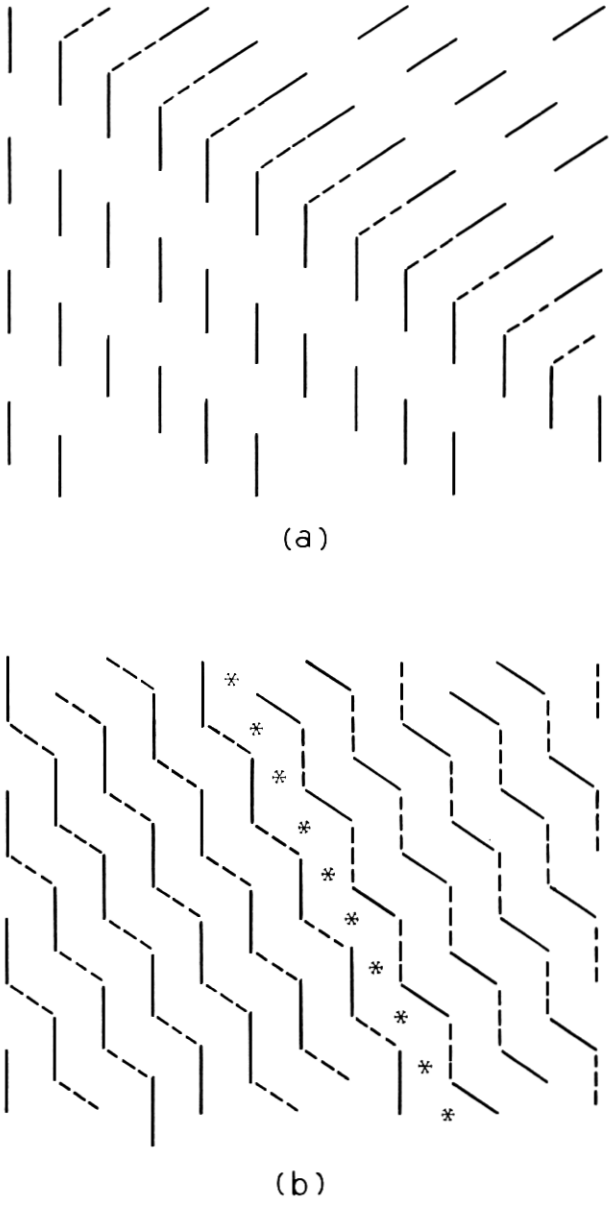

Fig. 13 — (a) $(200)[\frac{1}{2}\bar{\frac{1}{2}}0]:(1\bar{1}0)[\frac{1}{2}\bar{\frac{1}{2}}0]$ phase boundary; (b) $(200)\cdot(110)[\frac{1}{2}\frac{1}{2}0]:[\frac{1}{2}\frac{1}{2}0]i:(200)\cdot(110)[\frac{1}{2}\frac{1}{2}0]$ domain boundary.

The identity displacement from one fold surface to the next is $[\frac{1}{2}\frac{1}{2}0]$. The structure of fold surfaces might be written as $(200)\cdot(110)[\frac{1}{2}\frac{1}{2}0]$. A new type of domain boundary has been introduced into the middle of the figure parallel to (310). The fold structures in the two domains are identical except for an inversion *or* reflection across the (001) plane. On the left the (200) plane folds are on the upper surface, on the right they are on the lower surface, etc. There *may* be an array of inversion points along the boundary, and this possibility is indicated by asterisks in Fig. 13(b). If the domains are related by an inversion they will both have the same inclination to the basal plane. If the domains are related by reflection across (001) they will have opposite inclinations to the basal plane. In the event that the fold surfaces have a stacking sequence which forms a crystal surface tangent to (001) then, of course, there would be no distinction between inversion and reflection. There is a difference in surface energies between the upper and lower crystal surfaces. Whatever the difference in energies may be in the left-hand domain it will be reversed in the right-hand domain. Also, the binding energy between the two fold surfaces that comprise the domain boundary should be different from the binding energy between adjacent fold surfaces within a domain. The relation between the two fold surfaces at the boundary can be written as $[\frac{1}{2}\frac{1}{2}0]i$. The fold surface on the left is translated by $[\frac{1}{2}\frac{1}{2}0]$, followed by inversion between top and bottom, symbolized by i. The structure of Fig. 13(b) can then be written as

$$(200)\cdot(110)[\tfrac{1}{2}\tfrac{1}{2}0]:[\tfrac{1}{2}\tfrac{1}{2}0]i:(200)\cdot(110)[\tfrac{1}{2}\tfrac{1}{2}0].$$

IV. CHAIN FOLDING AND TWINNING

At the present time it appears that crystal aggregates of linear polyethylene may exhibit twinning on the (110), (310), (530) and (120) planes. There may well be other, as yet unobserved, twin planes. This remarkable versatility in twin formation must have a rational interpretation in terms of fold structures. In the preceding section it was required that the folds exhibit continuity at either domain boundaries or phase boundaries. The same condition of continuity must prevail at twin boundaries. However, the fold structures provide an additional variable that is not ordinarily encountered in twinning. Hence, for this discussion we define a twin to be a crystal aggregation that gives a diffraction pattern which is based on two identical reciprocal lattices with a definite crystallographic relation between them. This definition is used because we will consider aggregations in which there are two space lattices related by a twin law. The crystal structure with respect to the chains

and chain packing is identical on the two space lattices, but the fold structure is different on the two space lattices. The boundary between regions of such an aggregation will always be a twin boundary with respect to the space lattice and crystal structure inside the folds. However, with respect to the surface folds the boundary may be a domain boundary (a true twin boundary) or a phase boundary.

In the preceding section it was shown that boundaries in the fold structure may be formed either by an alteration in the stacking sequence of fold planes or by a change in orientation of the fold planes. Investigation of (110) twinning shows that each of these mechanisms can produce both domain boundaries and phase boundaries in the fold structure. Thus, there are four types of twinning to consider across a (110) boundary.

In Fig. 14 is illustrated an example of a change in stacking sequence to form a domain boundary. Expanding our previous notation, this can

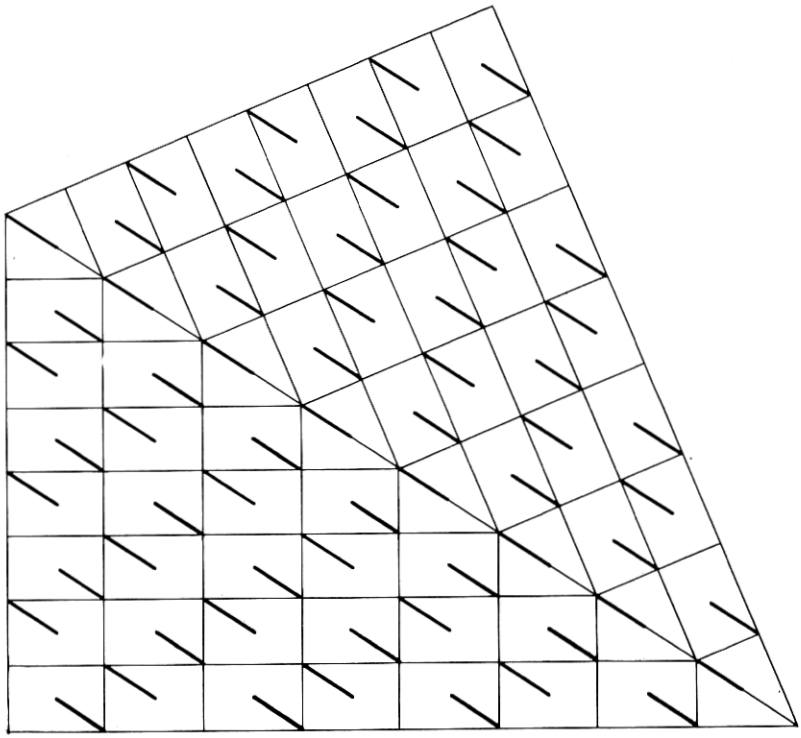

Fig. 14 — (110)[$\frac{1}{2}\frac{1}{2}$0]:(110):(110)[$\frac{1}{2}\frac{1}{2}$0] domain boundary in (110) twin.

be written as (110)[$\frac{1}{2}\frac{1}{2}$0]:(110):(110)[$\frac{1}{2}\frac{1}{2}$0], the middle (110) entry being added to indicate that the space lattices are twinned across the (110) plane.

In Fig. 15 the stacking sequence is altered to form a phase boundary. In this case the appropriate symbolism is (110)[010]:(110):(110)[$\frac{1}{2}\frac{1}{2}$0].

In Fig. 16 the fold plane changes orientation to form a domain boundary. The fold structure can be written as (1$\bar{1}$0)[$\frac{1}{2}\frac{\bar{1}}{2}$0]:(110):(1$\bar{1}$0)[$\frac{1}{2}\frac{\bar{1}}{2}$0].

In Fig. 17 the fold plane changes orientation to form a phase boundary. In this case the notation is somewhat more complex because of the stacking sequences: (200)[$\frac{1}{2}\frac{1}{2}$0]·[$\frac{1}{2}\frac{1}{2}$0]:(110):(1$\bar{1}$0)[0$\bar{1}$0]·[$\frac{1}{2}\frac{\bar{1}}{2}$0].

All told we have found 11 distinct fold structures across a (110) twin plane when we confine the original or left-hand member of the twin to the simple stacking sequences described in Section III. To save space, these structures are summarized in Table I in fold structure notation. It is possible to reconstruct a line drawing of any of these structures from the notation and the condition of continuity of the folds.

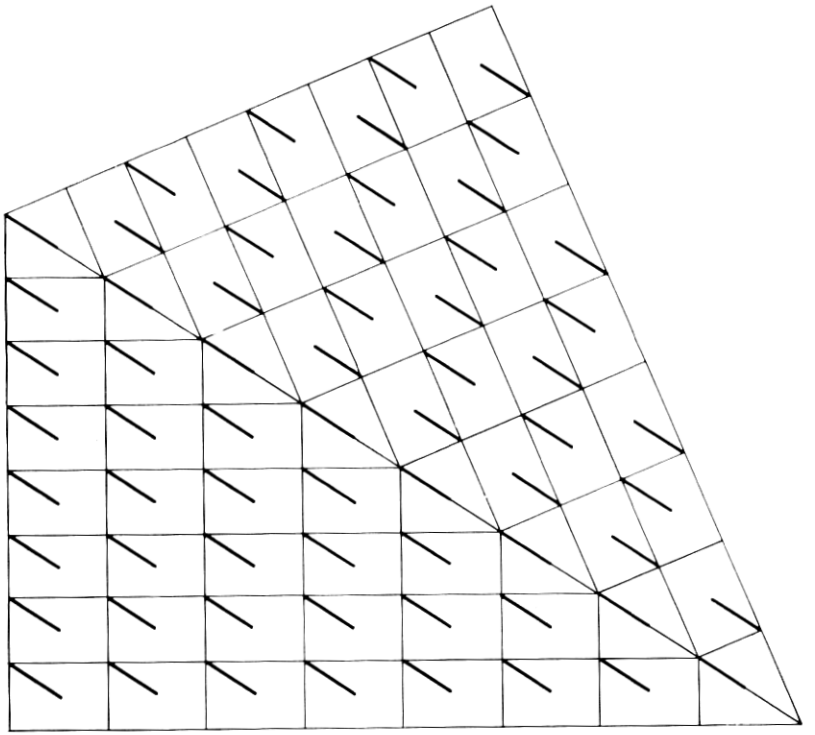

Fig. 15 — (110)[010]:(110):(110)[$\frac{1}{2}\frac{1}{2}$0] phase boundary in (110) twin.

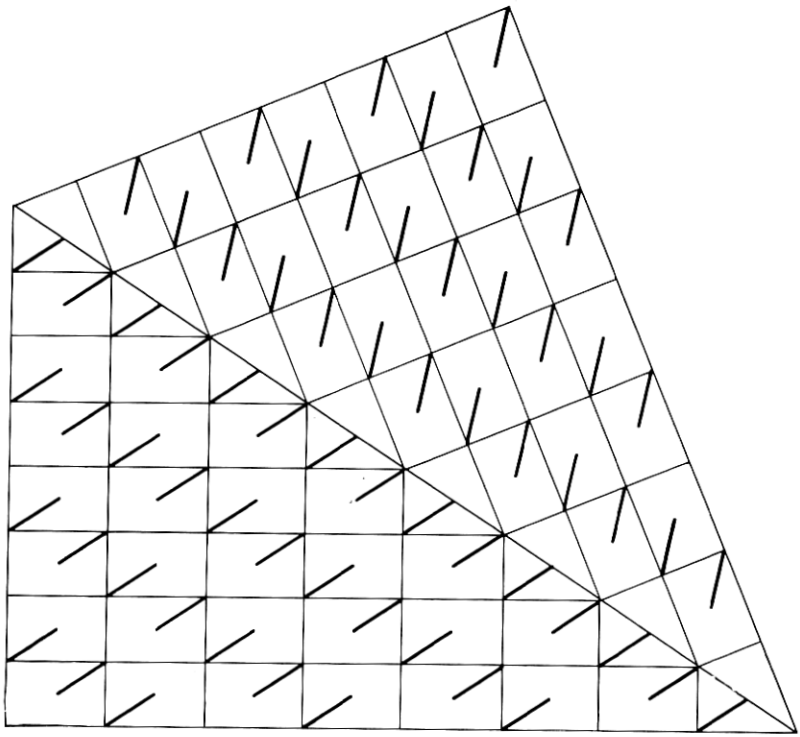

Fig. 16 — $(1\bar{1}0)[\frac{1}{2}\frac{\bar{1}}{2}0]:(110):(1\bar{1}0)[\frac{1}{2}\frac{\bar{1}}{2}0]$ domain boundary in (110) twin.

The formation of twin boundaries by a change in stacking sequence of fold planes is only possible for (110) twinning. In the case of (310) twinning both domain boundaries and phase boundaries can be formed by a change in orientation of the fold plane. Fig. 18 gives an example of a domain boundary. The change in orientation is extreme and an acute angle of 53°8′ is formed between a fold plane and its twinned extension. There is a pair of chains symmetrically disposed across the twin plane, one in the original fold plane, the other in the twinned extension, which are separated by 98.8 per cent of the normal packing distance. This slightly short packing distance occurs in all the (310) twins that will be discussed. In terms of the previous notation, the structure of Fig. 18 can be written as $(200)[\frac{1}{2}\frac{\bar{1}}{2}0]:(310):(200)[\frac{1}{2}\frac{\bar{1}}{2}0]$.

Fig. 19 is an example of a phase boundary. Here the change in orientation of the fold planes is almost negligible. In the usual notation, the structure is written as $(110)[010]:(310):(200)[\frac{1}{2}\frac{\bar{1}}{2}0]$.

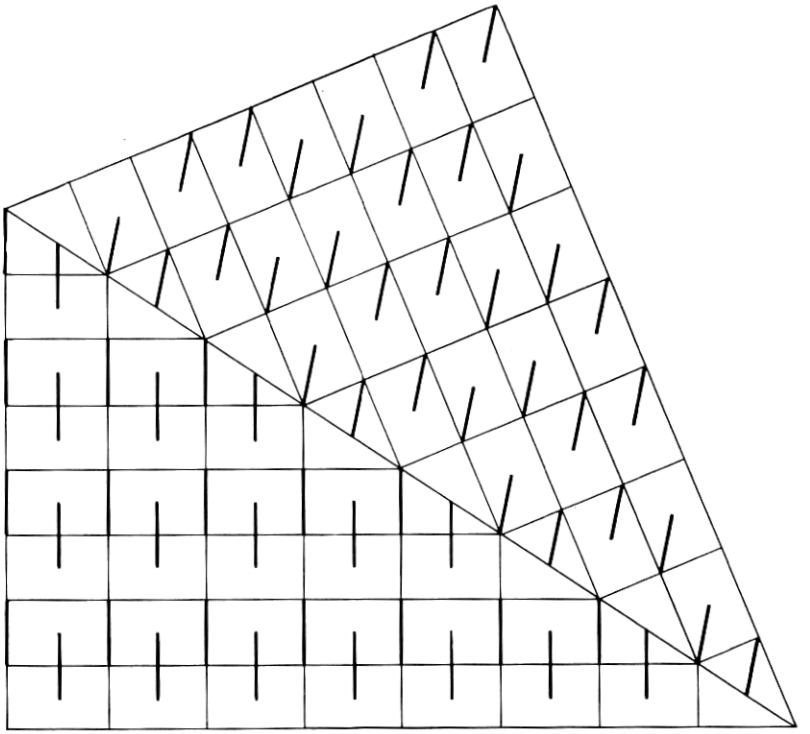

Fig. 17 — $(200)[\frac{1}{2}\frac{1}{2}0]\cdot[\frac{1}{2}\frac{\bar{1}}{2}0]:(110):(1\bar{1}0)[0\bar{1}0]\cdot[\frac{1}{2}\frac{\bar{1}}{2}0]$ phase boundary in (110) twin.

TABLE I—SOME GEOMETRICALLY POSSIBLE FOLD STRUCTURES IN (110) TWINNING

Change in Stacking Sequence of Fold Planes	
To form domain boundary	1. $(110)[\frac{1}{2}\frac{1}{2}0]:(110):(110)[\frac{1}{2}\frac{1}{2}0]$ 2. $(110)[010]:(110):(110)[010]$
To form phase boundary	3. $(110)[010]:(110):(110)[\frac{1}{2}\frac{1}{2}0]$
Change in Orientation of Fold Planes	
To form domain boundary	4. $(1\bar{1}0)[\frac{1}{2}\frac{\bar{1}}{2}0]:(110):(1\bar{1}0)[\frac{1}{2}\frac{\bar{1}}{2}0]$ 5. $(1\bar{1}0)[0\bar{1}0]:(110):(1\bar{1}0)[0\bar{1}0]$ 6. $(200)[\frac{1}{2}\frac{1}{2}0]:(110):(200)[\frac{1}{2}\frac{1}{2}0]$ 7. $(200)[\frac{1}{2}\frac{1}{2}0]:(110):(200)[\frac{1}{2}\frac{1}{2}0]$ 8. $(200)[\frac{1}{2}\frac{1}{2}0]\cdot[\frac{1}{2}\frac{\bar{1}}{2}0]:(110):(200)[\frac{1}{2}\frac{1}{2}0]\cdot[\frac{1}{2}\frac{\bar{1}}{2}0]$
To form phase boundary	9. $(200)[\frac{1}{2}\frac{1}{2}0]:(110):(1\bar{1}0)[010]$ 10. $(200)[\frac{1}{2}\frac{1}{2}0]:(110):(1\bar{1}0)[\frac{1}{2}\frac{\bar{1}}{2}0]$ 11. $(200)[\frac{1}{2}\frac{1}{2}0]\cdot[\frac{1}{2}\frac{\bar{1}}{2}0]:(110):(1\bar{1}0)[0\bar{1}0]\cdot[\frac{1}{2}\frac{\bar{1}}{2}0]$

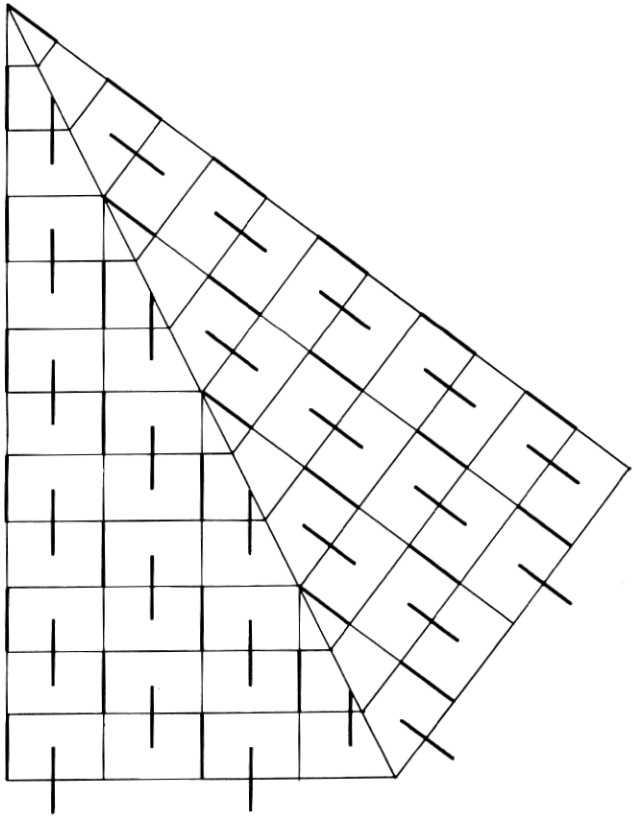

Fig. 18 — (200)[$\frac{1}{2}\bar{\frac{1}{2}}$0]:(310):(200)[$\frac{1}{2}\bar{\frac{1}{2}}$0] domain boundary in (310) twin.

Fig. 20 is still another phase boundary, which involves a new detail. Alternate fold planes contain a fold which does not terminate at the twin plane. Instead, this fold straddles the twin plane and has a fold width that is 98.8 per cent of the width of a (110) fold. The previous notation suffices to cover this detail as long as it is understood that the condition of continuity must be satisfied, and the structure is written as (1$\bar{1}$0)[010]:(310):(1$\bar{1}$0)[$\frac{1}{2}\bar{\frac{1}{2}}$0].

Nine distinct fold structures have been found when we confine the original or left-hand member of the twin to the simple stacking sequences. These structures are summarized in Table II.

An entirely different possibility for twin boundaries arises if we consider structures based on fold surfaces instead of fold planes Some of

the properties of a fold surface structure were discussed in connection with Fig. 13(b), and a more generalized structure is shown in Fig. 21. The twin on the left can be described by the symbol $(200)\cdot(110)[\frac{1}{2}\frac{1}{2}0]i$, where the notation $[\frac{1}{2}\frac{1}{2}0]i$ indicates that the displacement from a fold in one fold surface to an equivalent fold in the next fold surface involves the translation $[\frac{1}{2}\frac{1}{2}0]$ followed by an inversion between top and bottom. Since the folds of a given fold width alternate between top and bottom at alternate fold surfaces, there is no difference in the upper and lower crystal surface energies.

The twin on the right is described by the notation $(200)(110)[\frac{1}{2}\frac{1}{2}0]$, where now there *is* a difference in the upper and lower crystal surface energies. The relation between the two structures at the twin plane can

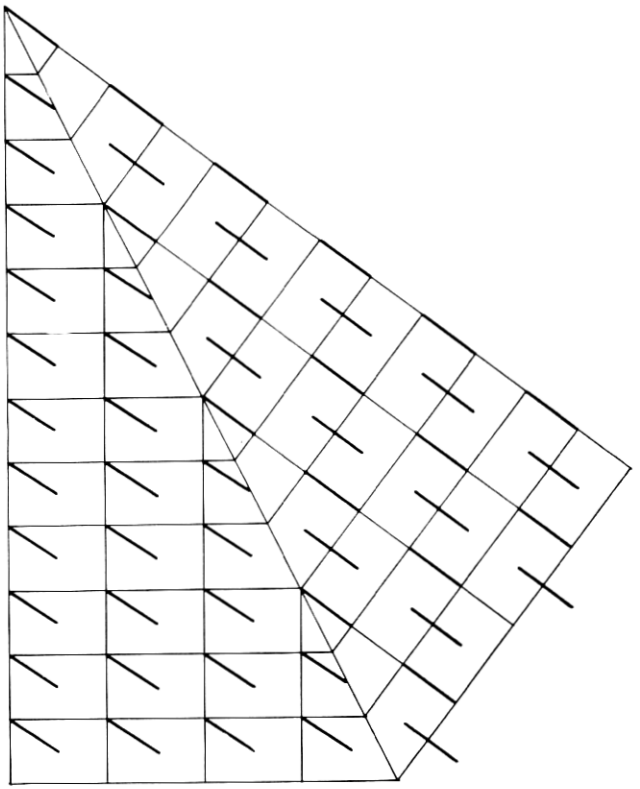

Fig. 19 — $(110)[010]:(310):(200)[\frac{1}{2}\bar{\frac{1}{2}}0]$ phase boundary in (310) twin.

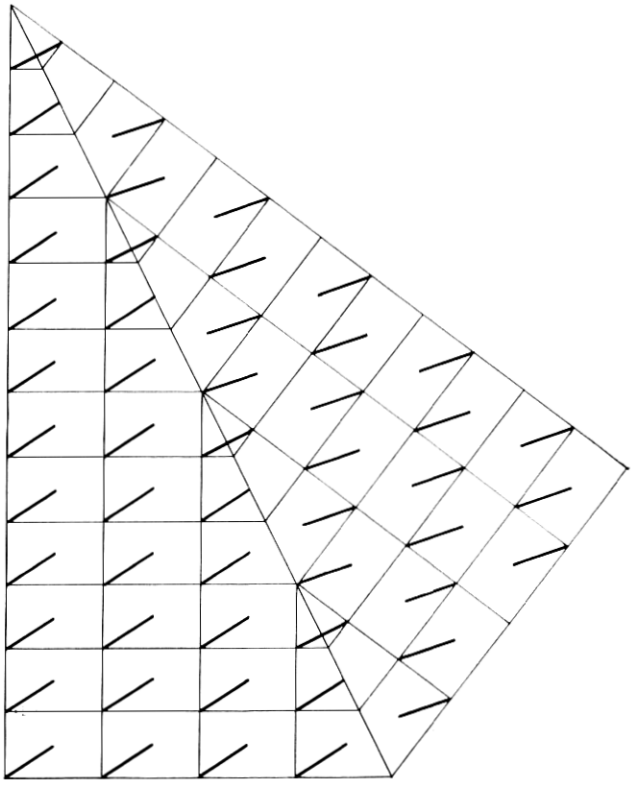

Fig. 20 — $(1\bar{1}0)[010]:(310):(1\bar{1}0)[\frac{1}{2}\frac{\bar{1}}{2}0]$ phase boundary in (310) twin.

be described by the symbol $(310)[0\bar{1}0]i$. The terminal fold surface in the left-hand twin is reflected across (310), placing it in the right-hand twin. This is followed by translation along $[0\bar{1}0]$ in the right-hand space lattice, and then by inversion between top and bottom. Each fold in the terminal fold surface of the left-hand twin has now been displaced to an equivalent fold in the terminal fold surface of the right-hand twin. The structure of Fig. 21 can then be written as

$$(200)\cdot(110)[\tfrac{1}{2}\tfrac{1}{2}0]i:(310)[0\bar{1}0]i:(200)\cdot(110)[\tfrac{1}{2}\tfrac{1}{2}0].$$

A total of six distinct fold structures are found when transformations of fold surfaces are considered. These are also summarized in Table II, making a total of 15 distinct fold structures across a (310) twin plane.

For (530) twinning, only one example has been found of a boundary

formed by a change in orientation of a fold plane. This example is illustrated in Fig. 22. It is similar to the structure of Fig. 20 in that it is a phase boundary and two thirds of the fold planes contain a fold which straddles the twin plane. The widths of these straddle folds are 145 per cent and 98.7 per cent of the width of a (110) fold. The latter slightly short packing distance occurs in all the (530) twins that will be discussed. In contrast to the structure of Fig. 20, there are pairs of vacant lattice sites which straddle the (530) boundary at regular intervals. These vacancies are inevitable if, in addition to the condition of continuity, we require that neighboring chains cannot be appreciably closer together than the width of a (110) fold. The structure of Fig. 22 can be written as $(200)[\frac{1}{2}\bar{\frac{1}{2}}0]:(530):(200)[\frac{1}{2}\bar{\frac{1}{2}}0]\cdot 2[\frac{1}{2}\frac{1}{2}0]$, where the notation $[\frac{1}{2}\bar{\frac{1}{2}}0]\cdot 2[\frac{1}{2}\frac{1}{2}0]$ indicates that a displacement of $[\frac{1}{2}\bar{\frac{1}{2}}0]$ is followed by two successive displacements of $[\frac{1}{2}\frac{1}{2}0]$.

When transformations of fold surfaces are considered, six more (530) boundary structures are obtained. An example of a domain boundary is given in Fig. 23. The fold surface is defined by a sequence of one fold in a (200) plane followed by three folds in a (110) plane. Thus, the fold surface might be written as $(200)\cdot 3(110)$. The transformation across the boundary involves reflection across (530), a translation of $[\bar{1}10]$ in

TABLE II — SOME GEOMETRICALLY POSSIBLE FOLD STRUCTURES IN (310) TWINNING

	Change in Orientation of Fold Planes
To form domain boundary	1. $(110)[\frac{1}{2}\frac{1}{2}0]:(310):(110)[\frac{1}{2}\frac{1}{2}0]$ 2. $(110)[010]:(310):(110)[010]$ 3. $(200)[\frac{1}{2}\frac{1}{2}0]:(310):(200)[\frac{1}{2}\frac{1}{2}0]$ 4. $(200)[\frac{1}{2}\bar{\frac{1}{2}}0]:(310):(200)[\frac{1}{2}\bar{\frac{1}{2}}0]$ 5. $(200)[\frac{1}{2}\frac{1}{2}0]\cdot[\bar{\frac{1}{2}}\frac{1}{2}0]:(310):(200)[\frac{1}{2}\frac{1}{2}0]\cdot[\bar{\frac{1}{2}}\frac{1}{2}0]$
To form phase boundary	6. $(110)[\frac{1}{2}\frac{1}{2}0]:(310):(200)[\frac{1}{2}\frac{1}{2}0]$ 7. $(110)[010]:(310):(200)[\frac{1}{2}\frac{1}{2}0]$ 8. $(1\bar{1}0)[010]:(310):(1\bar{1}0)[\frac{1}{2}\frac{1}{2}0]$ 9. $(200)[\frac{1}{2}\frac{1}{2}0]\cdot[\frac{1}{2}\bar{\frac{1}{2}}0]:(310):(110)[010]\cdot[\frac{1}{2}\frac{1}{2}0]$
	Transformation of Fold Surfaces
To form domain boundary	10. $(200)\cdot(110)[\frac{1}{2}\frac{1}{2}0]:(310)[0\bar{1}0]:(200)\cdot(110)[\frac{1}{2}\frac{1}{2}0]$ 11. $(200)\cdot(110)[\frac{1}{2}\frac{1}{2}0]i:(310)[0\bar{1}0]:(200)\cdot(110)[\frac{1}{2}\frac{1}{2}0]i$ 12. $(200)\cdot(110)[\frac{1}{2}\frac{1}{2}0]:(310)[0\bar{1}0]i:(200)\cdot(110)[\frac{1}{2}\frac{1}{2}0]$ 13. $(200)\cdot(110)[\frac{1}{2}\frac{1}{2}0]i:(310)[0\bar{1}0]i:(200)\cdot(110)[\frac{1}{2}\frac{1}{2}0]i$
To form phase boundary	14. $(200)\cdot(110)[\frac{1}{2}\frac{1}{2}0]i:(310)[0\bar{1}0]:(200)\cdot(110)[\frac{1}{2}\frac{1}{2}0]$ 15. $(200)\cdot(110)[\frac{1}{2}\frac{1}{2}0]i:(310)[0\bar{1}0]i:(200)\cdot(110)[\frac{1}{2}\frac{1}{2}0]$

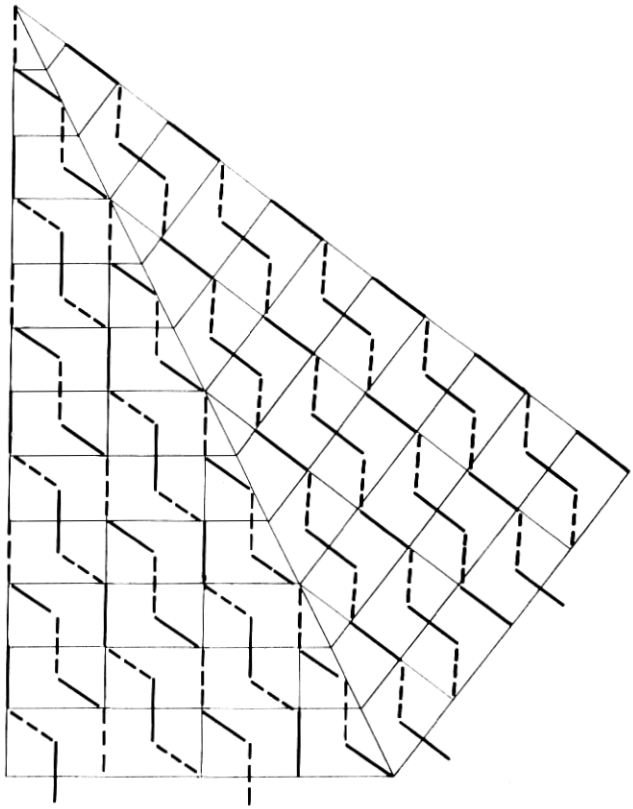

Fig. 21 — $(200)\cdot(110)[\frac{1}{2}\frac{1}{2}0]i:(310)[0\bar{1}0]i:(200)\cdot(110)[\frac{1}{2}\frac{1}{2}0]$ phase boundary in (310) twin.

the right-hand space lattice, and inversion. Hence the structure of Fig. 23 can be written as $(200)\cdot 3(110)[\frac{1}{2}\frac{1}{2}0]:(530)[\bar{1}10]i:(200)\cdot 3(110)[\frac{1}{2}\frac{1}{2}0]$. There are four domain boundaries and two phase boundaries based on fold surfaces, exactly as for the (310) boundaries listed in the lower part of Table II.

There is good evidence in Fig. 7 for the existence of (530) crystal faces. The existence of fold surfaces seems quite likely, both in terms of observed morphology and observed twin relations. The experimental evidence for (120) twinning is perhaps somewhat weaker. However, if (120) twin boundaries do exist the possibilities are quite analogous to the (530) case. One phase boundary has been found based on a change in orientation of a fold plane. There are boundary folds whose widths are 21.5 per cent and 5 per cent larger than the width of a (110) fold. The struc-

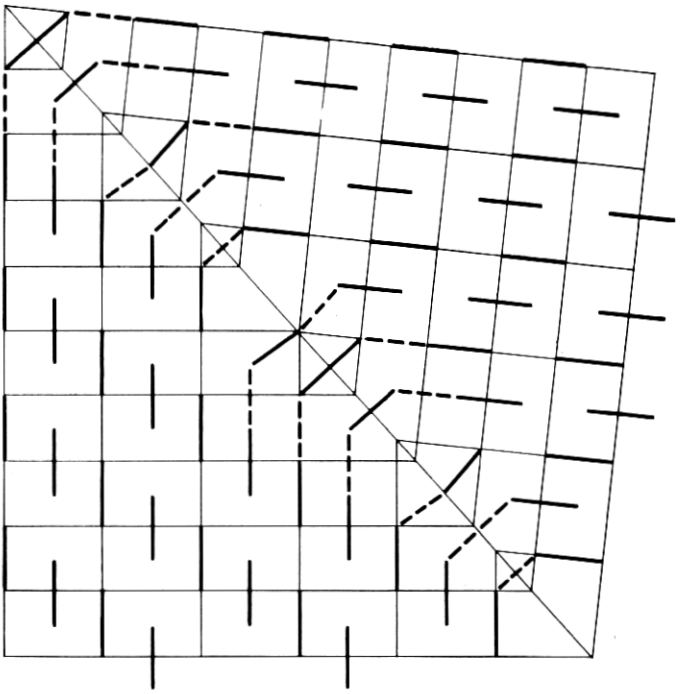

Fig. 22 — (200)[$\frac{1}{2}\frac{\bar{1}}{2}$0]: (530): (200)[$\frac{1}{2}\frac{\bar{1}}{2}$0]·2[$\frac{1}{2}\frac{1}{2}$0] phase boundary in (530) twin.

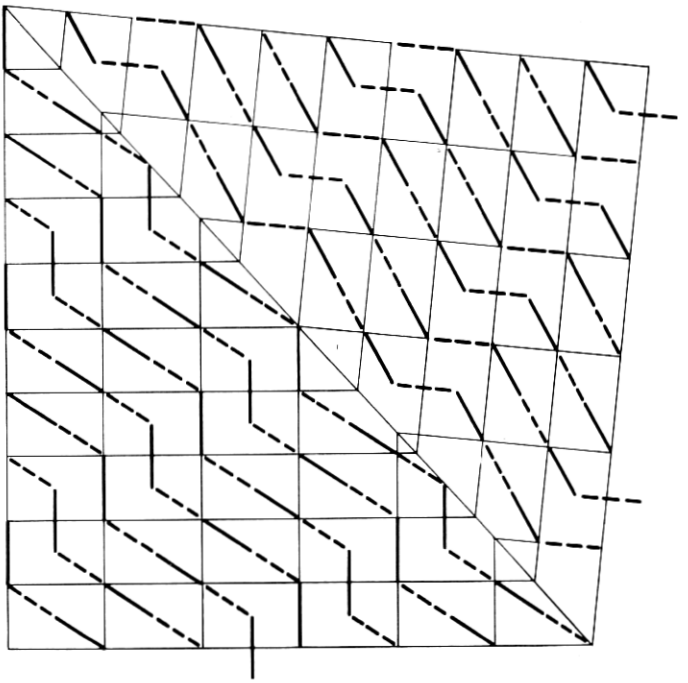

Fig. 23 — (200)·3(110)[$\frac{1}{2}\frac{1}{2}$0]: (530)[$\bar{1}$10]i: (200)·3(110)[$\frac{1}{2}\frac{1}{2}$0] domain boundary in (530) twin.

ture may be described as $(1\bar{1}0)[\frac{1}{2}\frac{\bar{1}}{2}0]:(120):(1\bar{1}0)[\frac{1}{2}\frac{\bar{1}}{2}0]\cdot 2[0\bar{1}0]$. There are four domain boundaries and two phase boundaries based on $(1\bar{1}0)\cdot 3(110)$ fold surfaces. For example, one of the domain boundaries is written as

$$(1\bar{1}0)\cdot 3(110)[010]:(120)[\bar{1}00]:(1\bar{1}0)\cdot 3(110)[010].$$

V. CHAIN FOLDING AND CRYSTAL GROWTH

In the previous sections various types of structures involving fold planes, fold surfaces, domain boundaries and phase boundaries have been discussed as they might arise in either a single space lattice or a pair of twinned space lattices. In all instances a small crystalline region has been abstracted out of a larger crystal. To place these geometrical abstractions in proper perspective, it is necessary to consider how fold structures develop during the process of crystal nucleation and growth. The three-dimensional aspects of crystal growth, especially the relatively constant chain length between folds, and the variation of fold length with temperature, have been treated in meticulous detail by Lauritzen and Hoffman.[14] In what follows attention will be directed to various factors whose significance is practically independent of lamellar thickness.

There are two basic ingredients in the formation of a two-dimensional crystal (i.e., a crystal which essentially covers a surface instead of filling a volume) with a chain fold structure. First, there must be a continuity of the fold structure which permits any molecule to add its folds to the existing fold structure without any special restrictions on the molecule as to its total unfolded length or its time sequence in the growth process. Second, the structure must develop in a way that permits each chain to possess the maximum number of nearest-neighbor chains consistent with the chain packing in the crystal structure.

The simplest lamellar structure that is consistent with the basic conditions laid down above is illustrated in Fig. 24. A dot at the center of the figure marks the initial fold at one end of a molecule. The fold plane changes orientation at the second fold, again at the third fold, fifth fold, seventh fold, and so on to maintain the maximum number of nearest-neighbor chains. As successive revolutions or loops are formed around the nucleus, a single spiral structure evolves in a clockwise direction. In Fig. 24 three molecules have been indicated, each containing 100 folds. A dot at the end of the fifth loop indicates the end of the first molecule and the beginning of the second. A dot at the end of the seventh loop indicates the end of the second molecule and the beginning of the third. Somewhat over half way around the ninth loop the third molecule

ends. The crystal contains four domains of the (110)[010] type, two domain boundaries of the (110)[010]:(1$\bar{1}$0)[010] type, and two domain boundaries of the (110)[010]:($\bar{1}$10)[010] type. This is the type of crystal that was described by Reneker and Geil[11] as forming either (001) or (111) crystal surfaces. It is apparent that there must be both a spiral structure and a continuity of the fold planes from one domain to the next. There is no good reason why the starting point of a crystal might not be a fold at some other point than the end of a molecule. In this case, a double spiral structure will be formed at the center. This will have consequences for the subsequent structure of the crystal which will be discussed below. Both single-spiral and double-spiral crystal nuclei were among the possibilities recognized by Lauritzen and Hoffman.

The structure of Fig. 24 provides a convenient model for some simple calculations that are not without physical insight. From the geometry of the fold structure, if the number of loops around the spiral at a given point in the growth be designated n, then the number of folds in the last or outer loop is $4(2n - 1)$. Assume a weight average molecular weight of 130,000 for the polymer; then an average molecule contains 9285 CH_2 units. Suppose there are 93 CH_2 units per chain plus fold, with 3 CH_2 units per fold and 90 CH_2 units per chain. Then with 2.53 angstroms along the c axis per pair of CH_2 units, the fold length is 114 angstroms. There are approximately 100 folds per molecule. With these assumptions the total number of molecules in the crystal at any stage of the crystal growth is determined by a count of the number of folds. In addition, the number of molecules in the outer five loops is $(2n/5) - 1$.

The rate of addition of molecules to the crystal will be proportional

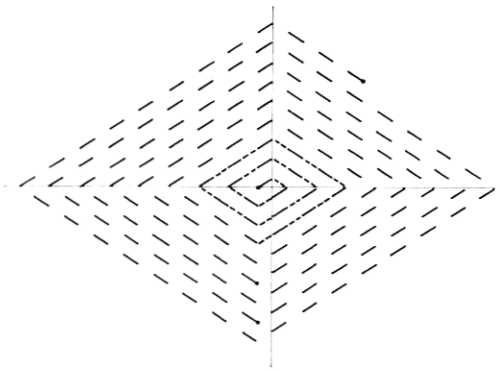

Fig. 24 — Single-spiral crystal containing (110)[010]-type fold domains. Dots indicate terminal points of three molecules included in figure.

to the average number of molecules in contact with the growing surface. This average number of molecules in turn is proportional to the area of the growing lateral faces of the crystal. The lateral area is proportional to the number of folds in the outer loop of the spiral. Thus, we can state that the average time for the formation of a fold on the growing surface is inversely proportional to $4(2n - 1)$, or

$$\text{time/fold} = \frac{K}{4(2n - 1)}.$$

Now assume that a crystal grows to 30μ in length along the a axis in 30 minutes. The number of loops encountered at various stages of the growth to 30μ size is listed in Table III, along with other time-independent quantities. The number of loops has grown to 20,480 when the crystal is about 30μ long. Now the constant K can be evaluated, since the time required for all the folds to form is

$$1800 \text{ seconds} = \sum_{n=1}^{n=20,480} \frac{K}{4(2n - 1)} [4(2n - 1)] = 20,480K,$$

or

$$K = \frac{1800}{20,480} = 0.08789 \text{ second.}$$

Based on the above assumptions, the average time per fold at various stages of growth is listed in Table III. Note that identical numerical values can be obtained by simply assuming that the same time interval is required to form each loop in the spiral. The quantity $5K = 0.439$ second is an interesting one, since it is the time required for an integral number of molecules to be added to form the outer five loops. The number of molecules varies from one in the first five loops to 8191 in the last five loops. The calculations completely ignore the question of the time required for the initial nucleation. Even so, the estimates of rate of fold formation or rate of addition of molecules should be reasonable for all but a few of the innermost loops of the spiral.

There is one detail of the growing spiral structure of Fig. 24 that requires further comment. Four times in every loop it is necessary to "round a corner." In each instance a fold has to project beyond the surface formed by the preceding loop. In Fig. 24 this occurs at the fourth, sixth, ninth, 12th, 16th, 20th, 25th, ... folds. Clearly there is an energy barrier that must be surmounted at each of these points. Lauritzen and Hoffman devoted considerable attention to this question.

However, there is more than one way in which a corner may

TABLE III — CRYSTAL GROWTH OF SINGLE-SPIRAL (110)[010] FOLD STRUCTURE

(Assuming Growth to 30μ Size in 30 Minutes)

Number of Loops, n	Number of Folds in Outer Loop, $4(2n-1)$	Number of Molecules in Crystal*	Length of Crystal	Number of Molecules in Outer 5 Loops,† $(2n/5)-1$	Average Time per Fold‡ (in seconds)
1	4	—	—	—	2.2×10^{-2}
2	12	—	—	—	7.3×10^{-3}
3	20	—	—	—	4.4×10^{-3}
4	28	—	—	—	3.1×10^{-3}
5	36	1	$6.7 \times 10^{-3}\mu$	1	2.4×10^{-3}
10	76	4	1.4×10^{-2}	3	1.2×10^{-3}
15	116	9	2.1×10^{-2}	5	7.6×10^{-4}
20	156	16	2.9×10^{-2}	7	5.6×10^{-4}
40	316	64	5.8×10^{-2}	15	2.8×10^{-4}
80	636	256	1.2×10^{-1}	31	1.4×10^{-4}
160	1,276	1,024	2.4×10^{-1}	63	6.9×10^{-5}
320	2,556	4,096	4.7×10^{-1}	127	3.4×10^{-5}
640	5,116	16,384	9.5×10^{-1}	255	1.7×10^{-5}
1,280	10,236	65,536	1.9	511	8.6×10^{-6}
2,560	20,476	262,144	3.8	1,023	4.3×10^{-6}
5,120	40,956	1,048,576	7.6	2,047	2.1×10^{-6}
10,240	81,916	4,194,304	1.5×10	4,095	1.1×10^{-6}
20,480	163,836	16,777,216	3.0×10	8,191	5.4×10^{-7}

* Number of folds in crystal = 100 (number of molecules in crystal) + 4, for all loops with $n > 5$.

† Outer five loops are formed in 0.439 second.

‡ Average time per molecule $\leqq$ 100 (average time per fold), for all loops with $n > 5$

be rounded. Consider the situation presented in Fig. 25. Again, there is a single spiral developing in a clockwise direction. At the fourth fold the corner has been rounded, not by adding another fold in a (110) plane but by adding a fold in a (200) plane. It may require more energy to form a (200) fold. However, the altered arrangement of nearest-neighbor and next-nearest-neighbor chains will make other adjustments in the energy balance. There are dozens of configurations that conceivably might arise in forming the first two or three loops of a single spiral nucleus. In Fig. 25 the spiral has been constructed in such a way that each loop has one interruption by a (200) fold. The result of this is to produce a $[\frac{1}{2}\frac{1}{2}0]$ stacking sequence of (110) fold planes. One may protest that a "jog" is produced in every loop where the (200) fold occurs. In Fig. 26 an alternative way of producing a single spiral $(110)[\frac{1}{2}\frac{1}{2}0]$ fold structure is shown. There is no jog in the loop pattern, but a sequence of vacancies has been produced along the $(\bar{1}10)[\bar{\frac{1}{2}}\frac{1}{2}0]:(\bar{1}\bar{1}0)[\frac{1}{2}\bar{\frac{1}{2}}0]$ domain boundary. This may appear to be an even more unlikely structure than the preceding one. The interesting fact is that it is impossible to produce a

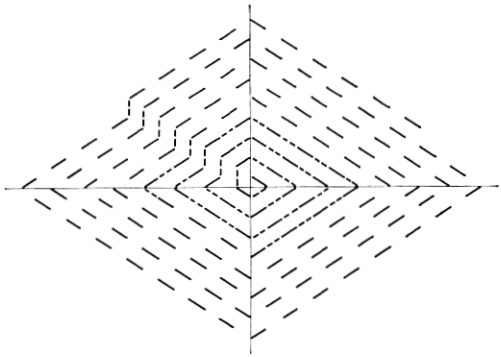

Fig. 25 — Single-spiral crystal containing (110)[$\frac{1}{2}\frac{1}{2}$0]-type domains. One (200) fold is required in every loop to maintain the stacking sequence.

single-spiral (110)[$\frac{1}{2}\frac{1}{2}$0] fold structure without introducing a (200) fold in each loop to maintain the [$\frac{1}{2}\frac{1}{2}$0] stacking sequence.

In Fig. 27 a clockwise double-spiral structure is illustrated. In this case a 115-fold molecule has been drawn at the center. The first fold in the nucleus is the 29th fold in the molecule. One branch of the double spiral contains 28 folds; the other contains 86 folds. As long as the two branches parallel each other, a (110)[$\frac{1}{2}\frac{1}{2}$0] structure is produced automatically. However, as soon as the long branch overlaps the short branch, the structure reverts to (110)[010]. If a second molecule adds to the crystal in single-spiral form the (110)[010] structure will continue, as illustrated in Fig. 27.

To produce an extensive double-spiral structure many coincidences

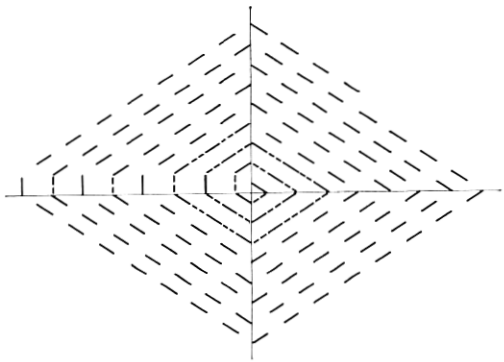

Fig. 26 — Single-spiral crystal containing (110)[$\frac{1}{2}\frac{1}{2}$0]-type domains. When the (200) folds are arrayed along the horizontal axis a vacancy is generated with each loop.

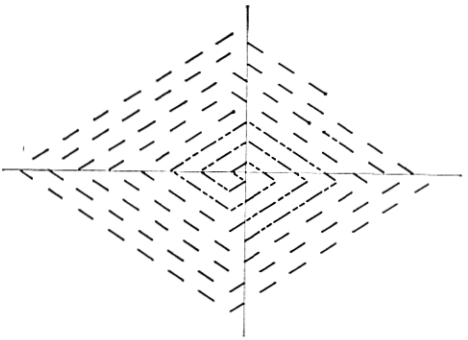

Fig. 27 — Double-spiral nucleus with first fold located 29 folds from one end of molecule. Monolayer nucleation and addition of a second molecule.

are necessary. The first fold in the nucleus must occur at the middle of a molecule. Later molecules must add as double monolayers with the first fold at the middle of the molecule. However, it is inconceivable that later molecules would not also add as two monolayers proceeding in both clockwise and counterclockwise directions. It seems very unlikely that an extensive (110)[$\frac{1}{2}\frac{1}{2}$0] structure can be produced from either single or double spirals, without introducing a systematic array of (200) folds into the structure as in Fig. 25.

Fig. 28 gives an indication of how complex and interwoven the relations between molecules may become, depending on their sequence in

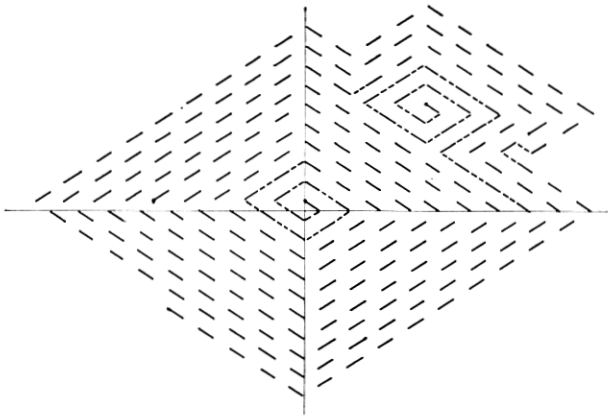

Fig. 28 — Single spiral (110)[010] structure, showing four molecules and spiral secondary nucleation of third molecule in time sequence.

time. There are four molecules included in the figure. At the center, a 100-fold molecule commences a single spiral (110)[010] structure. After five loops a 150-fold molecule continues the structure. By the time the second molecule has completed a loop and a half a new event occurs. A third 101-fold molecule has formed a secondary nucleus which has completed two loops and added on to the structural sequence. Now two monolayers of folds follow, one after the other, around the perimeter of the compound crystal. A fourth 100-fold molecule adds on where the 150-fold molecule terminates and continues on past the termination of the 101-fold molecule. If each molecule could be given a color, the perimeter of the crystal would appear like striped candy. Although an integral (110)[010] phase has been maintained throughout, the addition of the secondary nucleus is revealed by the presence of four new fold domains and six new domain boundaries.

If conditions are favorable for the presence of spiral secondary nuclei it is likely that they would be attracted to the innermost corners of the re-entrant faces. Hence, if a secondary nucleus adds to a sizable primary crystal, a whole string of secondary nuclei might be added, one after another. Such an array would lie in a virtually straight line if the time sequence were rapid. It is apparent that, as a crystal grows in size, whether from addition of secondary spirals or monolayers, traffic jams are bound to develop. Additions will occur in both clockwise and counterclockwise directions; there will be collisions with adjustments to make. Under such conditions one would expect a variety of fold surfaces and other space lattice orientations to become more probable as a crystal aggregate develops.

A great diversity of fold structures can occur in a single spiral and still satisfy the condition of continuity. A suggestion of the possibilities is indicated in Fig. 29. The figure contains ten molecules varying in length from 30 folds to 100 folds. Many different phase boundaries have arisen within a lamella of relatively simple external shape. The precise conditions which determine how a corner shall be rounded are the decisive factor in determining the fold structure. The first molecule forms folds in (200) planes at the fourth and eighth folds. A phase domain based on (200)·(110) fold surfaces develops in a radial direction from the fourth fold. This domain has boundaries tangent to (110), $(1\bar{3}0)$, and $(\bar{1}\bar{1}0)$ planes. Proceeding in a radial direction from the eighth fold, a pair of vacancies are followed by a domain based on (200) fold planes. This domain has boundaries tangent to (110), $(1\bar{1}0)$, $(\bar{1}\bar{1}0)$, and $(\bar{1}10)$ planes. Most of the area of the crystal is filled in with (110) fold planes. However, the stacking sequences are irregular because of the varying numbers of (200) folds that occur in the different loops.

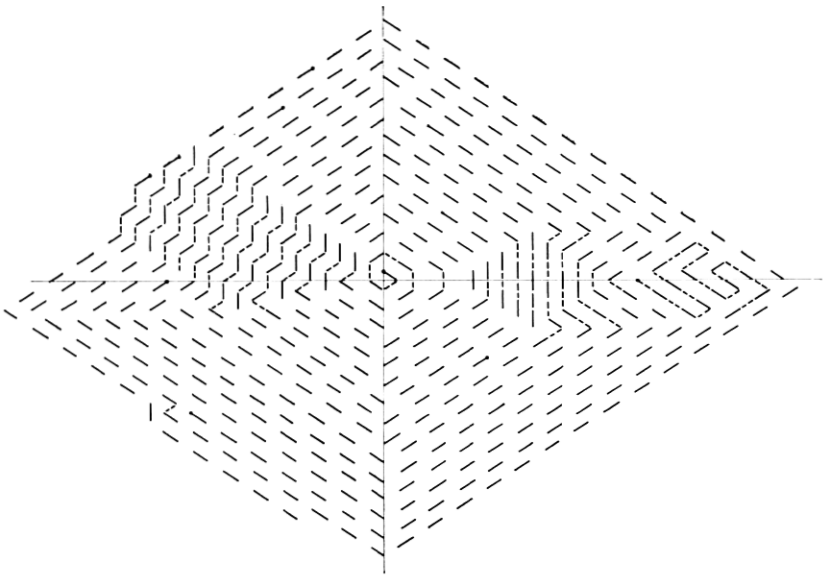

Fig. 29 — Hypothetical single-spiral crystal containing a variety of phase boundaries and domain boundaries, and showing ten molecules.

A pair of re-entrant faces are developed from the (200) fold domain. The inner corner formed by these faces would be expected to be a likely nucleation site. Suppose the experimental conditions are such that secondary nuclei of the monolayer type are favored. Then, to fill in the re-entrant area, a molecule would need to develop in a maze-like pattern such as is indicated in Fig. 29. However, this process should be very time-consuming because of the frequency with which corners must be rounded. Such a factor may offer a partial explanation for the widespread occurrence of re-entrant faces in many crystal aggregates.

VI. ELECTRON INTERFERENCE EFFECTS

The diversity and complexity of fold structures discussed in the preceding sections suggest an explanation for the types of electron interference effects which are illustrated in Figs. 5, 6 and 7. Whenever there is a change from one structure or domain to another, the associated crystal surface is likely to change its inclination to the (001) plane.

Certain restraints are placed on the morphology by the requirement of continuity across boundaries combined with a spiral growth process. The simplest possible loop around a spiral involves crossing four domain boundaries as in Fig. 24. Each domain is part of the same phase and

the displacement of successive fold planes along c can be identical in each domain. Surface forces between crystal and solution are symmetric on the upper and lower crystal surfaces. Perfect continuity can be achieved in this simple crystal without imposing any strain.

In a more complicated crystal, such as in Fig. 29, the situation is quite different. For example, the sixth loop around the spiral involves crossing four phase boundaries and two domain boundaries. The 12th loop involves crossing five phase boundaries and four domain boundaries. When successive domains belong to different phases the displacement of successive fold planes or fold surfaces along c will not in general be identical in each domain. In addition, the surface forces between crystal and solution will vary. There will be a change in surface energy in crossing a phase boundary at either the upper or lower crystal surfaces. For some phases there will be a difference in surface energy between upper and lower crystal surfaces within a single phase domain, as indicated in Figs. 13(b), 21 and 23. In achieving continuity around the loop the changes in surface orientations that occur in crossing boundaries must either add up to zero for a full revolution or be compensated by a strain pattern. As a complex structure develops, the crystal surfaces are likely to contain both discreet changes in orientation along well-defined crystallographic directions and continuous warpings or curvatures in both tangential and radial directions.

When a crystal is removed from solution and the solvent is allowed to evaporate still other changes may be expected. The distribution of surface tensions will be quite different for a crystal in air as opposed to those for a crystal in xylene. Adjustments in surface morphology are inevitable, and such effects as collapsed hollow pyramids and doubled-up lamellae may arise from such factors.

When electron interference effects give rise to contrast lines along well-defined directions, it is reasonable to suppose that in many instances they delineate phase boundaries or domain boundaries. When the contrast appears along curves or loops, continuous warpings or curvatures are being revealed. It is a moot point whether these nonlinear effects can be directly correlated with the position of boundaries. It is not unreasonable to think that they do indicate the occurrence, if not the actual position, of boundaries. The interpretation is bound to be complicated by extraneous deformations introduced in the process of drying and manipulating crystals for examination. With a limited number of experimental observations it is not reasonable to attempt more than a qualitative relation between interference effects and fold structure. With sufficient experimental data it becomes quite plausible that a definite cor-

relation could be obtained between a given contrast line and a specific type of phase or domain boundary.

VII. ACKNOWLEDGMENTS

I am very grateful to Miss S. Eloise Koonce, who patiently instructed me in the basic operation of the Siemens Elmiskop I. Many members of the chemistry department provided me with polymer materials, preprints and abstracts, encouragement and interest. I am especially indebted to J. B. Howard, J. L. Lundberg, W. P. Slichter and F. H. Winslow for their many courtesies.

REFERENCES

1. Till, P. H., The Growth of Single Crystals of Linear Polyethylene, J. Polymer Sci., **24,** 1957, p. 301.
2. Keller, A., A Note on Single Crystals in Polymers: Evidence for a Folded Chain Configuration, Phil. Mag., **2,** 1957, p. 1171.
3. Fischer, E. W., Stufen- und spiralförmiges Kristallwachstum bei Hochpolymeren, Z. Naturf., **12a,** 1957, p. 753.
4. Storks, K. H., An Electron Diffraction Examination of Some Linear High Polymers, J. Am. Chem. Soc., **60,** 1938, p. 1753.
5. Keller, A., and O'Connor, A., Study of Single Crystals and Their Associations in Polymers, Disc. Far. Soc., No. 25, 1958, p. 114.
6. Agar, A. W., Frank, F. C. and Keller, A., Crystallinity Effects in the Electron Microscopy of Polyethylene, Phil. Mag., **4,** 1959, p. 32.
7. Sella, C., and Trillat, J. J., Structures Périodiques dans les Polyéthylènes, C. R. Acad. Sci. Fr., **248,** 1959, p. 410.
8. Bassett, D. C., Frank, F. C., and Keller, A., Evidence for Distinct Sectors in Polymer Single Crystals, Nature, **184,** 1959, p. 810.
9. Niegisch, W. D., The Nucleation of Polyethylene Spherulites by Single Crystals, J. Polymer Sci., **40,** 1959, p. 263.
10. Niegisch, W. D. and Swan, P. R., Pyramidal Single Crystals of Polyethylene, Bull. Am. Phys. Soc., **5,** 1960, p. 192.
11. Reneker, D. H. and Geil, P. H., Morphology of Polymer Single Crystals, Bull. Am. Phys. Soc. **5,** 1960, p. 193.
12. Belavtseva, E. M., The Law of Mutual Substitution for the Process of Disordering of Some Crystal Compounds Under the Action of Moderate-Energy Electrons, Doklady Akad. Nauk SSSR, **125,** 1959, p. 1005.
13. Dowell, W. C. T., Farrant, J. L., and Rees, A. L. G., Electron Interference in Lamellar Crystals, Proc. Int. Conf. Electron Microscopy, London, 1954, p. 279.
14. Lauritzen, J. I., Jr. and Hoffman, J. D., Theory of Formation of Polymer Crystals with Folded Chains in Dilute Solution, J. Research, Natl. Bur. Standards, **64A,** 1960, p. 73.